Synthesis and structural characterization of $AlPO_4$-18 and Magnesium and Zinc substituted $AlPO_4$-18

Mahesh Bhagwat, C. V. V. Satyanarayana and Veda Ramaswamy*
Catalysis Division, National Chemical Laboratory, Pune 411008, India

Abstract

$AlPO_4$-18, $MgAlPO_4$-18 and $ZnAlPO_4$-18 have been synthesized by using N, N-di-isopropyl ethylamine as the structure directing agent. The powder XRD data of the metal substituted samples show significant changes in the patterns as an effect of metal loading. The metal loaded samples show broader peaks (smaller crystallite size) and lower crystallinity as compared to the $AlPO_4$-18. Indexing the powder patterns revealed that AEI sample has the space group C2/c. The MAPO-18 samples showed lowering of symmetry with a change in the space group to $P2_1$. An increase in the lattice parameters of the Zn and Mg substituted samples is observed which indicates isomorphous substitution of metals in the aluminophosphate framework. The solid state ^{27}Al NMR data confirmed substitution of the metal atoms in the Al site, preferentially at the Al-1 site. The ^{31}P NMR data indicate formation of one more crystallographically different P atom as an effect of metal loading.

Key words: $AlPO_4$-18, MAPO-18, XRD, NMR, Zinc, Magnesium

Tel. No.: +91 +20 589 3400 Fax No. –91+20 589 3761
E-mail: veda@cata.ncl.res.in

1. Introduction

$AlPO_4$-18 has been widely studied ever since Wilson et al [1] first reported its synthesis about two decades ago. It is a microporous crystalline aluminophosphate molecular sieve with a chabazite-like structure having pear shaped pores . The aluminophosphate framework gives rise to a three dimensional pore system with an average pore diameter of 4.3 Å. Substitution of lower valent metal atoms in the aluminophosphate framework has been reported for a wide range of metal atoms. A variety of metals like Zn, Mg, Ni, Cu Co, Fe and Mn have been incorporated in the $AlPO_4$-18 framework [2-4]. Incorporation of these lower valent metal ions imparts a net negative charge to the otherwise neutral framework, which makes the material interesting for catalytic applications. These metal substituted molecular sieves have been characterized using various techniques to study the redox behavior of the substituted metal atom. However, very few reports are available which report the structural features of these materials [5-9]. These small pore aluminophosphates with chabazite structure are excellent catalysts for the conversion of methanol to olefins [10-16]. Metal substituted $AlPO_4$-18 has been found to be active for selective functionalization of linear alkanes [17]. Because of the growing applications of these small pore structures, which were not considered as good catalysts earlier, these materials have now started

drawing the attention of catalysis researchers.

In the present study we have synthesized $AlPO_4$-18 and magnesium and zinc incorporated $AlPO_4$-18 samples (M = 5 and 10 mole % with respect to Al) by using N, N-di-isopropyl ethylamine as the structure-directing unit The crystal structure of the $AlPO_4$-18 sample has been reported by McCusker et al. However no reports of the structural features of the metal substituted materials could be found. Hence, an attempt has been made to study the effect of metal loading on the structural features of the aluminophosphate material, which play a significant role in its catalytic properties. The as-synthesized samples have been characterized by thermal analysis to study the thermal decomposition behavior of the template. All the samples have been characterized by powder XRD and solid state NMR spectroscopy to throw light on the structural changes taking place as a result of metal loading.

2. Experimental

2.1. Synthesis

The AlPO-18 and the metal incorporated samples were prepared using N, N-di-isopropyl ethylamine as the template by the hydrothermal route. A homogeneous gel was prepared by adding pseudo-boehemite to ortho-phosphoric acid. To the mixture, was added source of Mg/Zn (metal acetates) with continuous stirring. A typical gel composition for 10% Zn loading was $1P_2O_5$: 0.2ZnO: $0.9Al_2O_3$: 1.7TEMPLATE: $55H_2O$. Similarly, gels with 5 and 10% mole ratios of Mg and Zn were prepared. The samples were then heated in a Teflon coated stainless steel autoclave at 433 K in an oven. After 6 days, the samples were removed from the oven, washed thoroughly with water and centrifuged. The crystals were dried in an oven at 383 K for 12 h. The samples were then calcined in the furnace in air flow at 823 K for 24 h. The samples with 5 and 10 mole percent Zn and Mg are labeled as ZAP-5, ZAP-10, MAP-5 and MAP-10 respectively. The neat $AlPO_4$-18 sample is labeled as AEI.

2.2. Characterization

Chemical analysis of the samples was carried out to determine the metal content in the metal substituted samples. The samples were dissolved in minimum quantity of conc. HCl and the solutions were analyzed by Atomic Absorption Spectroscopy using a Perkin Elmer spectrometer.

The thermogravimetric analysis and the differential thermal analysis experiments were performed to study the decomposition behavior of the as-synthesized samples. Thermal analysis was done on a Setaram thermal analyzer (SETARAM) at a heating rate of 10 K min^{-1} in air atmosphere from room temperature to 1273K.

All the samples were scanned on a Rigaku D-Max III VC Powder X-ray Diffractometer using a Ni filter, Cu-Kα radiation (λ=1.5406Å) and NaI scintillator. Silicon was used as the internal standard to correct the 'd-spacing'. The samples were scanned in the step scan mode in the 2θ range, 20-100° with a step size of 0.02°. A counting time of 20 sec was employed per step. Crystallite size of the samples was determined by using the Scherrer equation, $L= k\lambda/B\cos\theta$ [18]. Crystallinity was determined by calculating the integrated area under the

peaks. The powder patterns were indexed using ITO and TREOR indexing programs to determine the unit cell parameters.

MAS NMR spectra were recorded in a Bruker DRX 500 spectrometer operating at a field of 11.6 Tesla. ^{27}Al spectra were recorded at a frequency of 130.3 mHz, with a pulse length of 2s and a spinning speed of 8-10 kHz. ^{31}P spectra were recorded at a frequency of 202.45 MHz with pulse length of 1.5s and a recycle delay of 4 sec.

3. Results and Discussion

3.1. Chemical analysis

The chemical analysis obtained by the Atomic Absorption Spectrophotometer showed presence of 5 and 9.27 mole % Mg and 5 and 9.85 mole % Zn in the MAP5, MAP10, ZAP5 and ZAP10 samples respectively. The data indicates complete substitution of the Mg and Zn added in the synthesis mixture.

3.2. Thermal analysis

Fig. 1 gives the multiple plots of the TG and the DTG analyses of the as-synthesized samples. The differential thermal analysis plots of the samples are given in Fig. 2. Table 1 gives the weight losses and the corresponding temperature range for all the samples. The thermogram of the AEI sample shows a total weight loss of about 19.8 % due to removal of water and the decomposition of the template in five major steps. The first weight loss is observed in the region 298 to 471 K. The differential thermogram shows a broad endothermic peak in this region that corresponds to the removal of water on the surface and from inside the pores of the aluminophosphate. The second step of the thermogram shows a weight loss

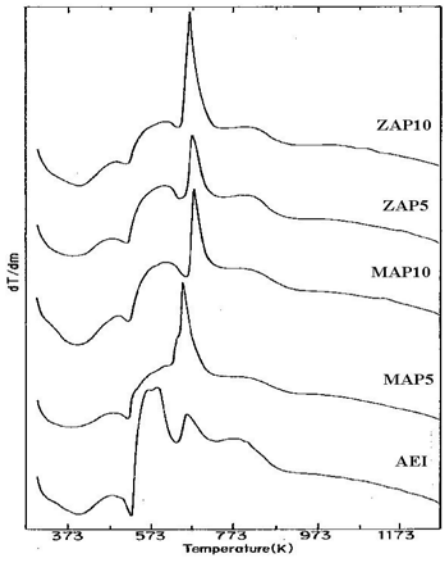

Fig. 1 Multiple plots of the thermograms and the differential thermograms plots of $AlPO_4$-18 and Zn and Mg substituted of $AlPO_4$-18.

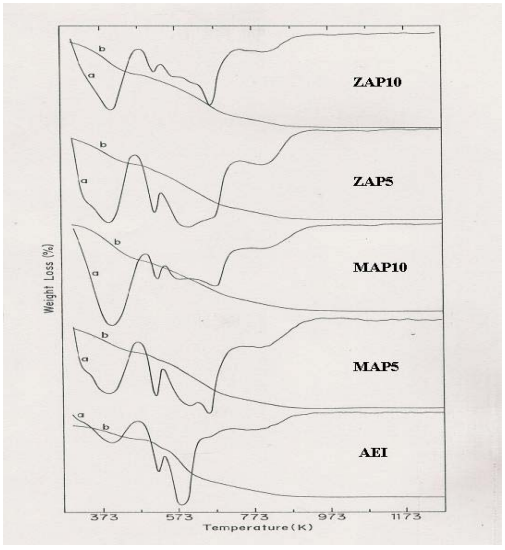

Fig. 2 Multiple plots of the differential thermal analysis curves of $AlPO_4$-18 and Zn and Mg substituted of $AlPO_4$-18.

in the region 472 to 646 K. The corresponding endothermic peak suggests loss of the physisorbed amine (used as the template). The weight loss in three steps between 541 and 646 K, 645 and 734 K and 735 and 909 K is continuous. The DTA curve indicates three corresponding exothermic peaks. The weight loss in the first two of these steps could be due to the decomposition of the protonated amine followed by the combustion of coke between the high temperature region 735-909 K. It can be observed that the weight loss in the region between 646 and 734 K due to the decomposition of the protonated amine is more for the MAP5 sample than that for the AEI sample. It can be observed that the amount of weight loss in this region corresponding to the template decomposition increases with the amount of metal incorporated into the aluminophosphate framework. This indicates isomorphous substitution of the metal atoms in the framework [17].

Table 1: TG data on metal incorporated aluminophosphates

Tempt. Range (K)	Weight loss due to	AEI	MAP5	MAP10	ZAP5	ZAP10
		% Weight loss				
298 – 471	Desorption of water	4	7.1	7.6	9.5	10.4
471- 646	Desorption of physisorbed amine	11.1	7.4	8.5	6.8	7.9
646 – 734	Decomposition of the protonated amine	2.2	3.9	5.3	2.4	4.5
734 – 1036	Coke combustion	2.5	2.5	2.8	2.6	2.9
	Total weight loss, %	19.8	20.9	24.2	21.3	25.7

3.3. Powder XRD analysis

Fig. 3 shows the powder XRD pattern of the as synthesized AlPO-18 sample. The pattern of the neat $AlPO_4$-18 (AEI) sample matched perfectly with the one reported in literature (10). The sharp reflections with high intensities indicate high crystallinity of the sample. The XRD patterns of the metal substituted samples (Fig. 4) also resembled that of $AlPO_4$-18. However, close examination of the XRD patterns revealed that the patterns of MeAPO-18 showed some small but significant differences. There are some additional peaks in the XRD patterns of all the MeAPO-18 samples. The powder patterns of the metal substituted samples show broader peaks. Also, a change in the relative intensities of some of the peaks is observed. These changes in the XRD are indicated in Fig. 4. Due to these differences in the patterns, all the profiles were indexed to obtain information about the unit cell parameters. The neat $AlPO_4$-18 sample pattern was indexed to obtain a monoclinic crystal system with unit cell parameters a = 18.477 Å, b = 12.598 Å, c = 13.554 Å, β = 95.129 ° and V = 3142.38 ($Å^3$). The crystal system showed a space group C2/c, the one reported in literature. Indexing of the patterns of the MeAPO-18 samples

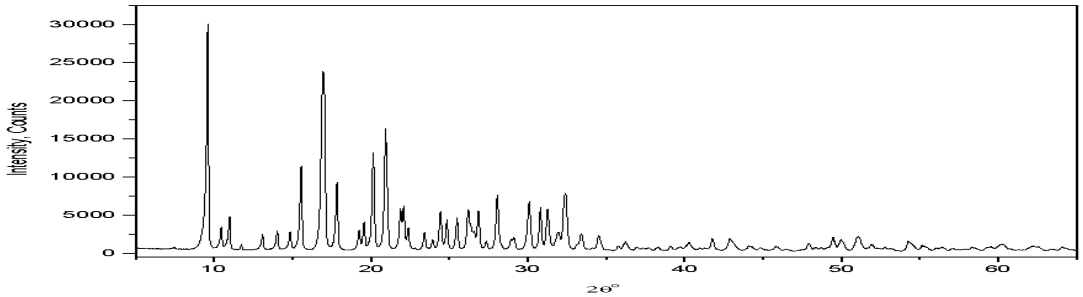

Fig. 3 The powder XRD pattern of the as synthesized AlPO-18 sample.

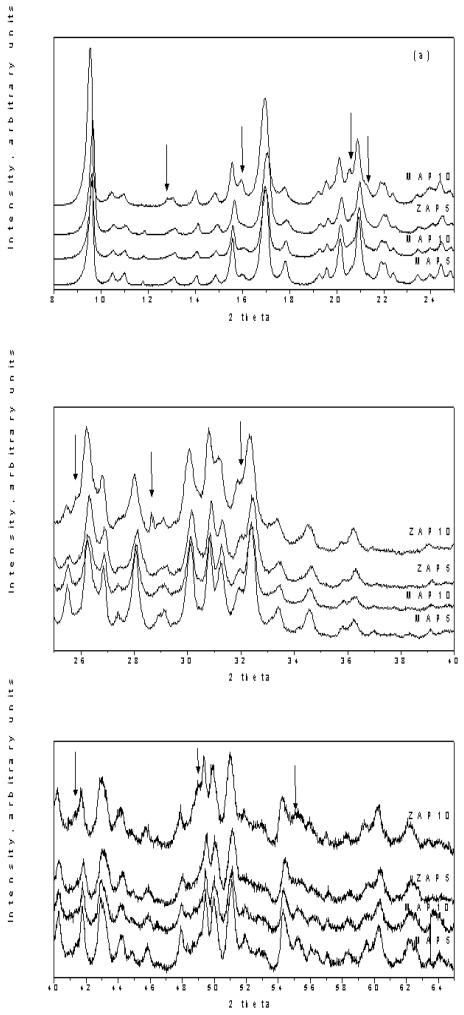

Fig. 4 Multiple plots of the powder XRD patterns of Zn and Mg substituted $AlPO_4$-18.

also showed presence of monoclinic crystal system. However, lowering of symmetry was observed, with the space group changing from C2/c to $P2_1$. The unit cell parameters, percent crystallinity with respect to the AEI sample and the crystallite size are reported in Table 2. The data indicate a decrease in the crystallinity of the metal incorporated samples (with respect to AEI) with increase in the amount of metal loading. Also a decrease in the crystallite size can be seen as an effect of metal loading. Isomorphous substitution of the metal ions in the $AlPO_4$-18 framework is confirmed by the change in the lattice parameters of the samples. An increase in the unit cell parameters is observed with the increase in concentration of Mg as well as Zn in the metal substituted samples.

3.4. NMR analysis

The ^{27}Al NMR spectrum of the neat $AlPO_4$-18 and the metal substituted samples are given in Fig. 5. The spectrum of the neat $AlPO_4$-18 sample matches with the one reported in literature. The spectrum shows three resonance peaks at 45, 39 and 9.8 ppm. The first peak is very narrow and symmetric. The second peak is a little

Table 2: The crystallographic information obtained from the powder XRD data of $AlPO_4$-18 and the Zn and Mg substituted $AlPO_4$-18.

	Space group	Unit cell parameters					Crystalli-nity	Crystallite size, nm
		a (Å)	b (Å)	c (Å)	V ($Å^3$)	β (°)		
AEI	C2/c	18.477	12.598	13.554	3142.38	95.129	100	572
MAP5	$P2_1$	18.463	12.585	13.542	3134.05	95.079	85	41
MAP10	$P2_1$	18.471	12.591	13.551	3139.65	94.972	79	34
ZAP5	$P2_1$	18.482	12.603	13.556	3144.57	95.203	83	38
ZAP10	$P2_1$	18.489	12.606	13.561	3148.52	95.03	74	31

broader whereas the third peak is very broad like a typical quadrupolar powder patterns. The three peaks indicate three crystallographically different Al sites. The peaks at 45 and 39 ppm can be assigned to 4 co-ordinate Al (Al-1 and Al-2, respectively) while that at 9.8 ppm can be assigned to 5 co-ordinate Al (Al-3) [7]. The difference in line shapes of the peaks indicates difference in symmetries around the Al atoms. The ^{27}Al spectra of the 5 and 10 % metal (Zn and Mg) substituted AEI samples also show three peaks each at similar positions. There is a decrease in the intensity of the peak at 45 ppm in the MAP5 sample. There is a further decrease in the intensity of this peak at 10% metal loading of Mg. This suggests substitution of Mg in the aluminophosphate framework preferentially at Al1 site. Similar trend can be observed for the 5% and 10% zinc-substituted samples. For the 10% zinc substituted sample, intensity of the peak at 39 ppm is more than that of the peak at 45 ppm. This clearly indicates the substitution of Zn in the framework at Al1 site. These trends also suggest that zinc is more effectively substituted in the framework than Mg. The broadening of the peak at 9.8 ppm suggests distortion in the symmetry of the 5-coordinated Al, which seems to increase with the increase in the metal content. Fig. 5 shows the ^{31}P NMR spectra of all the samples. The ^{31}P NMR spectra of the neat AlPO-18 sample shows three peaks at –18, -34 and –35 ppm, which are equal in intensities. They correspond to three crystallographically different 4 coordinated P atoms. The peak at –18 ppm is sharp while those at –34 and –35 ppm overlap. The ^{31}P NMR spectra of the metal substituted AEI samples show interesting results. The ^{31}P NMR of the ZAP5 and MAP5 samples show a decrease in the relative intensity of the peak at –18 ppm than the other two peaks as compared to the neat sample. The relative intensity of the peak at –35 ppm is more than that of the peak at –34 ppm in the neat $AlPO_4$-18 sample. In the metal substituted sample the reverse can be observed. Further the increase in the intensity of the peak at –34 ppm than the one at –35 ppm increases with the increasing metal content. These differences in intensities of the peaks in the spectra of the metal substituted AEI as compared to the neat sample suggest a change in environment of all the three P atoms. This observation confirms substitution of the metal in the

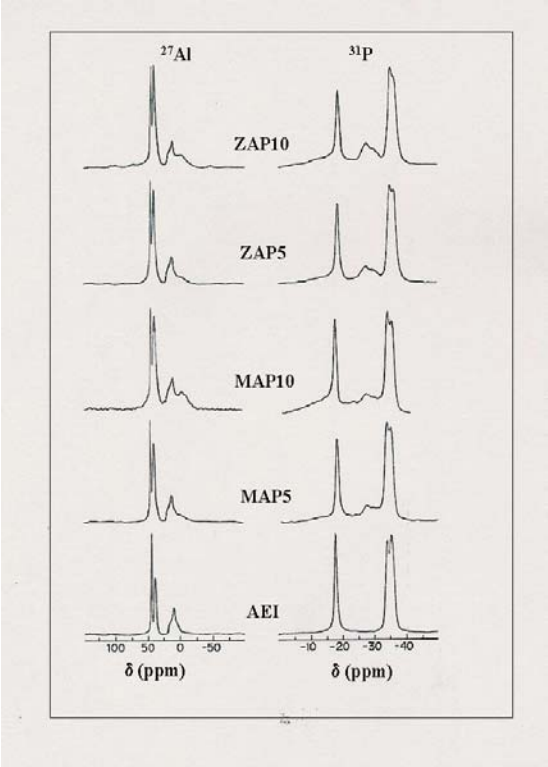

Fig. 5 The ^{27}Al and ^{31}P MAS NMR spectra of the neat $AlPO_4$-18 and the Zn and Mg substituted samples.

framework at the Al sites. An additional peak can be observed at –26 ppm in the spectra of the metal substituted samples. The intensity of this peak can be observed to increase with the increasing metal loading. This peak suggests presence of one more crystallographically different P atom in the metal substituted samples. This P atom could be the one adjacent to the metal atoms occupying the Al-1 site.

4. Conclusions

$AlPO_4$-18 and zinc and magnesium incorporated $AlPO_4$-18 (upto 10 mole % metal loading) can be synthesized by using N, N-di-isopropyl ethylamine as the structure directing agent. A decrease in crystallinity as well as the crystallite size of the sample is observed as a result of metal loading. While the $AlPO_4$-18 sample has the space group C2/c, the MAPO-18 samples showed lowering of symmetry with a change in the space group to $P2_1$. An increase in the lattice parameters of the Zn and Mg substituted samples confirms isomorphous substitution of the metal atoms in the aluminophosphate framework. The solid state ^{27}Al NMR data indicate substitution of the metal atoms in the Al site, preferentially at the Al-1 site. The ^{31}P NMR data confirms this and reveals formation of one more crystallographically different P atom as an effect of metal loading.

Acknowledgements

The authors are thankful to Dr. S. Ganapathy and Ms. Anuji Ebrahim for the NMR data and Dr. A.V.Ramaswamy for constant encouragement. The authors acknowledge the financial support of Department of Science and Technology, New Delhi for carrying out this work.

References

[1] S.T. Wilson, B. M. Lok, E. M. Flanigen, U.S. Patent No. 4,310, 1982, 440.
[2] L. Marchese, E. Gianotti, N. Damilano, S. Coluccia, J.M. Thomas, Catal. Lett., 37 (1996), 107.
[3] T. Wasowickz, S. J. Kim, S. B. Hong, L. Kevan, J. Phys. Chem., 100 (1996) 15954.
[4] P. A. Barrett, G. Sankar, R. H. Jones, C. Catlow, A. Richard, J. M. Thomas, J. Phys. Chem. B, 101 (1997) 9555.

[5] A. Simmen, L.B. McCusker, C. Baerlocher, W.M. Meier, Zeolites, 11 (1991) 654.
[6] Jochen Janchen, et. al., J. Phys. Chem., 97 (1996) 374.
[7] He, Heyong, Klinowski, Jacek, J. Phys. Chem., 97 (1993) 10385.
[8] A. Buchholz, W. Wang, M. Xu, A. Arnold, M. Hunger, Microporous and Mesoporous Materials 56 (2002) 267
[9] C. Jiesheng, J.M. Thomas, J. Chem. Soc., Chem. Commun., 5 (1994) 603.
[10] C. Jiesheng, J.M. Thomas, S. Gopinathan, J. Chem. Soc. Faraday Trans., 90 (1994) 3455.
[11] C. Jiesheng, J.M. Thomas, P.A. Wright, Catal. Lett., 28 (1994) 241.
[12] C. Jiesheng, J.M. Thomas, S. Gopinathan, J. Phys. Chem., 98 (1994), 10216.
[13] R. Wendelbo, D. Akporiaye, A. Andersen, I.M. Dahl, H.B. Mostad., Appl. Catal., A, 142 (1996) L197.
[14] J. Chen, P.A. Wright, S. Natarajan, J. M. Thomas, Stud. Surf. Sci. Catal., 84 (1994) 1731.
[15] R. Wendelbo, D. E. Akporiaye, A. Andersen, I. M. Dahl, H. B. Mustad, T. Fuglerud, S. Kvisle, Int. Appl. WO 9815496 A1 16 Apr 1998, 34 pp.
[16] M. A. Djieugoue, A. M. Prakash, L. Kevan, J. Phys. Chem. B, 104 (2000) 6452.
[17] R. Fernandez, M.V. Giotto, H.O. Pastore and D. Cardoso, Microporous and Mesoporous Materials 53 (2002) 135.
[18] X-ray diffraction Procedures: For polycrystalline and amorphous materials Eds: H.P. Klug and L.E. Alexander, (1974) John Wiley and Sons, New York. pp.618.